Mechanism for etching of exfoliated graphene on substrates by low-energy electron irradiation from helium plasma electron sources

John D. Femi-Oyetoro,[1] Kevin Yao,[1] Runtian Tang,[2] Phillip Ecton,[1] Kevin Roccapriore,[1] Ashley Mhlanga,[1] Guido Verbeck,[3] Duncan L. Weathers,[1] and Jose M. Perez[1,a)]
[1]*Department of Physics, University of North Texas, Denton, Texas 76203*
[2]*Department of Mechanical and Energy Engineering, University of North Texas, Denton, Texas 76203*
[3]*Department of Chemistry, University of North Texas, Denton, Texas 76203*

(Received 8 November 2018; accepted 12 February 2019; published 26 February 2019)

The authors investigate the mechanism for etching of exfoliated graphene multilayers on SiO_2 by low-energy (50 eV) electron irradiation using He plasma systems for electron sources. A mechanism for this etching has been previously proposed in which the incident electrons traverse the graphene and dissociate oxygen from the SiO_2 substrate at the graphene/SiO_2 interface. The dissociated oxygen reacts with carbon defects formed by the electron irradiation and thereby etches the graphene from below. They study etching using graphene flakes of various thicknesses on SiO_2, low and higher resistivity Si, indium tin oxide (ITO), and silicon carbide (SiC). They find that thicker layer graphene on SiO_2 does not etch less than thinner layers, contrary to the previously proposed model. They find that etching does not occur on low-resistivity Si and ITO. Etching occurs on higher resistivity Si and SiC, although much less than on SiO_2. This is attributed to He ion sputtering and vacancy formation. From these observations, they propose that oxygen etches graphene from above rather than below. In addition, they propose He ions instead of incident electrons cause the defects that oxygen reacts with and etches. *Published by the AVS.* https://doi.org/10.1116/1.5080445

I. INTRODUCTION

Graphene has attracted considerable interest due to its potential applications in electronics.[1] Etching is widely used in the fabrication of graphene device structures. We investigate the etching of exfoliated graphene on SiO_2 due to wide-area low-energy (LE) electron irradiation at 60 eV and dosages of about 0.7 C/cm^2. This type of etching has been reported when using electron sources based on plasma systems in which He gas is used.[2] A mechanism by which such etching occurs has been proposed in which the incident LE electrons travel through the graphene, dissociate oxygen from the SiO_2 substrate at the graphene/SiO_2 interface, and the dissociated oxygen etches the graphene from below.[2] However, details of the etching mechanism are not well known. Our objective is to better understand the mechanism by studying the effect of LE irradiation on other substrates such as low- and high-resistivity Si, indium tin oxide (ITO), and silicon carbide (SiC). The effects of irradiation are studied using optical microscopy and atomic force microscopy (AFM). Our results provide new insights into the physical basis of the mechanism.

Various methods have been reported for etching graphene such as reactive ion etching.[3–5] Techniques have also been developed to etch multilayer graphene one layer at a time, such as mild nitrogen[6] and oxygen[7] plasma exposure, sequential oxidation,[8] and laser thinning.[9] Also, focused high-energy electron[10] and helium ion[11] beams have been used for direct etching of graphene in which etching occurs due to knock-on collisions. The threshold electron energy for knock-on collision in graphene is about 86 keV,[12] and thus the energies at which LE electron irradiation etching occurs (50–200 eV) are below this threshold. Chen *et al.*[2] proposed that etching occurs during LE electron irradiation due to dissociation of oxygen from the SiO_2. It is known that an LE electron can excite bonds within a molecule such as SiO_2 to antibonding or nonbonding states, causing dissociation at thresholds of 15–20 eV.[13] In Ref. 2, it was proposed that the incident electrons go through the graphene layers, and the dissociated oxygen atoms etch the graphene by reacting with carbon bonds that have been damaged by the incident electrons. Etching of exfoliated graphene flakes consisting of up to about 13 layers was observed at electron energies of 50 eV and dosages of about 30 C/cm^2 deposited over a time period of 30 min. In addition, etching of amorphous carbon films 4–20 nm thick deposited on SiO_2 was also reported at incident electron energies of 200 eV and similar dosages. It was also reported that amorphous carbon films exhibited etching on SiO_2 but not Si substrates, and thus it was concluded that oxygen desorption from an oxygen containing substrate was required for etching to occur on carbon films including exfoliated graphene. We note, however, that electron irradiation of electrically isolated graphene flakes on dielectrics can result in negative graphene charging due to the low emitted secondary and backscattered electron yields from graphene and carbon films, as discussed below. Negative sample charging can result in the attraction of He^+ ions onto the surface, and such an ion bombardment may produce defects that play a role in the etching. Interestingly, in a paper by Lehtinen *et al.*,[14] numerical calculations are reported that show that He ion bombardment of graphene sheets causes the greatest amount of single vacancy defects and sputtering at low energies of around 30–80 eV. Defect formation by He ion bombardment proceeds by momentum transfer and in-plane recoil of carbon atoms.[14] Therefore, it is of interest to study the etching mechanism in more detail.

[a)]Author to whom correspondence should be addressed: jperez@unt.edu

 0734-2101/2019/37(2)/021401/7/$30.00

II. EXPERIMENT

Our experimental setup and procedures are described in detail in Refs. 15 and 16. A sketch of the system is shown in Fig. 1. Samples are mechanically exfoliated from highly oriented-pyrolytic graphite using the scotch tape method. A remote RF capacitively coupled plasma system with He gas at a pressure of 50 mTorr is used to generate the electrons.[15,16] The substrate is biased at +60 V attracting incident electrons at energies of about 60 eV.[16] We previously used this system to report the removal of single layers from exfoliated graphene by LE electron irradiation.[15] Chen *et al.*[2] used a mirror-confinement electron cyclotron resonance plasma system with He gas at 1.5×10^{-4} Torr to generate electrons at 50 eV. They state that He gas was used as the working gas to avoid the effect of ion impact on the carbon surface.[2] Helium ions would be formed as a result of electrons impacting He gas atoms. The use of plasma electron sources was necessitated by the need to expose the samples to high electron dosages on the order of 1–30 C/cm^2 during a reasonable exposure period of about 30 min.

The SiO_2 substrate was thermally grown to a thickness of 300 nm on a 500 μm thick Si (100) wafer with a resistivity of 0.01–0.02 Ω cm. The low-resistivity Si substrate was obtained from a 250 μm thick n-type Si (100) wafer with a resistivity of <0.005 Ω cm. The higher resistivity Si sample was obtained from an Si wafer with a resistivity of about 10 Ω cm. The native oxides of the wafers were removed by dipping them in a solution of HF acid. The electron irradiation experiments were carried out shortly after oxide removal. During this time, oxide layers of about 2–4 Å are estimated to have grown on the Si.[17] The ITO was sputtered to a thickness of 100 nm from a bulk piece of 90% In_2O_3 and 10% SnO_2 (90/10) ITO onto a substrate consisting of a 10 nm thick Al_2O_3 film sputtered onto a low-resistivity 250 μm thick Si substrate. The SiC was obtained from Thin Film Devices, Inc.[18] and was 300 nm thick and deposited on an Si substrate.

III. RESULTS AND DISCUSSION

Figure 2(a) shows an optical image of an exfoliated flake on 300 nm SiO_2 on Si containing regions of various thicknesses. As is known for this oxide thickness, few-layer graphene appears light purple due to interference effects, while successively thicker regions appear darker, and totally reflecting regions appear yellow.[1] Figure 2(b) shows an optical image of the flake after exposure for 10 min at a substrate bias of +60 V and a dosage of about 0.7 C/cm^2. After exposure, the few-layer regions have disappeared, and the intermediate regions appear lighter. Figures 2(c) and 2(d) show AFM images taken before and after the exposure, respectively. Figure 2(e) shows a height versus distance plot before (i) and after (ii) exposure taken along the line drawn in Fig. 2(d). As shown in Fig. 2(e), before exposure, the bright (yellow) and adjacent dark (purple) regions have heights of about 55 and 15 nm, respectively. After exposure, the bright (yellow) and dark (purple) regions have decreased in height to about 40 and 5 nm, respectively. Figure 2(f) shows a higher resolution AFM image of the 40 nm thick region after exposure showing wide round features on the surface that are characteristic of etching. We note that since the mean free path of electrons at 60 eV is about 0.48 nm,[19] one would expect significantly more electrons to reach the graphene/SiO_2 interface under the 15 nm thick region than under the 55 nm thick region. If the etching were due to oxygen atoms dissociated at the graphene/SiO_2 interface, as in the model proposed in Ref. 2, then more etching should occur for the 15 nm region than the 55 nm region. However,

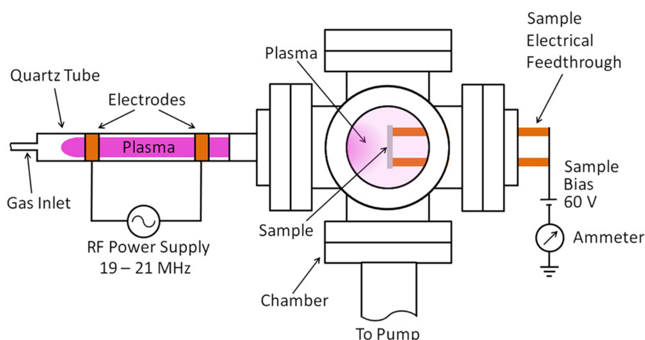

Fig. 1. Sketch of experimental setup, not drawn to scale. The plasma is ignited within the quartz tube by a 50 W power supply capacitively coupled by two copper electrodes outside the tube. The sample is placed at a working distance of about 20 cm from the center of the excitation region between the electrodes. The electrode spacing is about 10 cm. The sample is biased at +60 V to attract electrons from the plasma, and the current is measured by the ammeter.

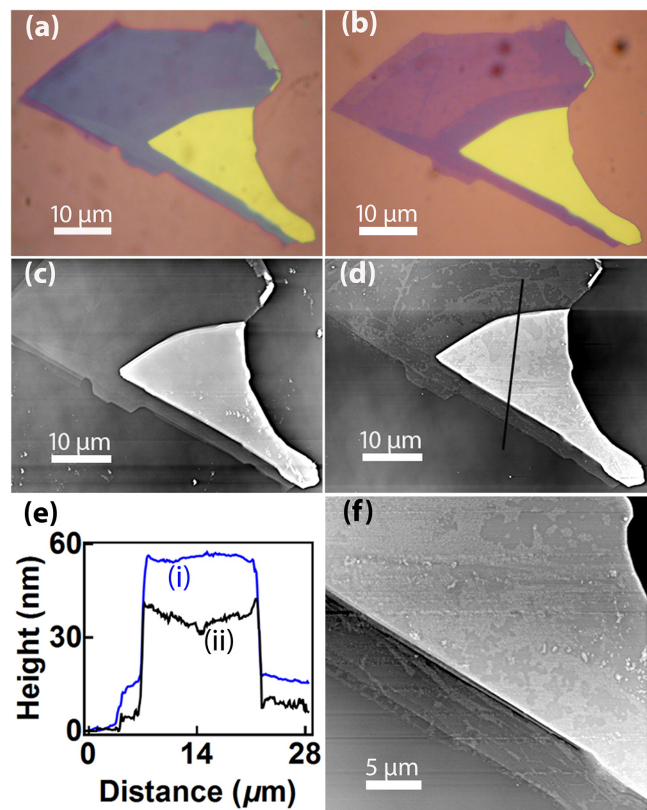

Fig. 2. Optical images of a graphene flake on SiO_2 (a) before and (b) after 10 min of electron exposure to a dosage of 0.7 C/cm^2. (c) and (d) AFM images before and after exposure, respectively. (e) Height profiles of the graphene flake before and after the exposure along the line drawn in (d). (f) AFM image of the thick bright (yellow) region from (d).

the 15 nm thick region etches by 10 nm, while the 55 nm region etches by 15 nm. Secondly, from the wide, round features observed in the AFM images, etching appears to have occurred on top of the flake. If the etching were due to oxygen atoms dissociated from underneath the flake, then the oxygen would have to diffuse 55 nm through the graphene to reach the top surface. However, theoretical studies have shown that oxygen atoms do not diffuse normal to the graphene surface and react at defect sites,[20] and exfoliated graphene is relatively defect-free. Therefore, these results support that etching occurs from above the sample instead of the graphene/SiO_2 interface. If oxygen plays a role in etching, then we propose that it mainly dissociates from the surrounding SiO_2 substrate, diffuses to the exfoliated graphene, and etches it from above. We do not know why the sample in Fig. 2 preferentially etches at the center of the flake. It may be due to diffusion or charging effects. However, the preferential etching at the center is a small effect.

We then irradiated an exfoliated flake on the low-resistivity Si substrate to test the oxygen dissociation hypothesis. Figure 3(a) shows an AFM image of a graphene flake before any irradiation. The height of this flake is about 60 nm as shown by Fig. 3(d), which is comparable to the thick flake on SiO_2 discussed previously in Fig. 2. Figure 3(b) shows an AFM image of the same flake after 10 min of exposure under the same irradiation conditions as those of Fig. 2. Figure 3(c) is another AFM image of the same flake after an additional 10 min of exposure under the same conditions as before, bringing the total exposure time of the sample to 20 min. Figure 3(d) shows the height profiles of the three AFM images all taken along the line scan indicated by the line drawn in Fig. 3(a). These height profiles are horizontally displaced for clarity, and they show no observable differences in height, indicating that the thick flake of graphene has not etched. We further corroborated our results by measuring a thin flake of graphene on a different area of the same substrate containing the thick graphene flake in Fig. 3. Figure 4(a) is an AFM image of a 13 nm graphene flake before irradiation, with a height comparable to the thin graphene sample on the SiO_2 substrate shown in Fig. 2. Figure 4(b) is an AFM image of the same thin flake after 10 min of irradiation. Figure 4(c) is an AFM image of the same sample after an additional 10 min of exposure. The height profiles of all three AFM images along the line in Fig. 4(a) are superimposed and shown in Fig. 4(d). As with Fig. 3(d), these lines are displaced horizontally for clarity. The height of the graphene flake remains at approximately 13 nm despite the 10 and 20 min of irradiation, indicating that thin samples on low-resistivity Si also do not etch. Chen *et al.*[2] concluded that the oxygen for etching comes from the SiO_2 and not from O_2 or H_2O gases in the chamber or adsorbates on the sample surface based on their observation that thin carbon films etch when deposited on SiO_2 but do not etch when deposited on Si. Our results that exfoliated graphene etches on SiO_2 but does not etch on low-resistivity Si support the conclusion that the oxygen comes from the SiO_2. In addition, Chen *et al.*[2] annealed the samples before irradiation at 400 °C for 30 min in the chamber under flowing He

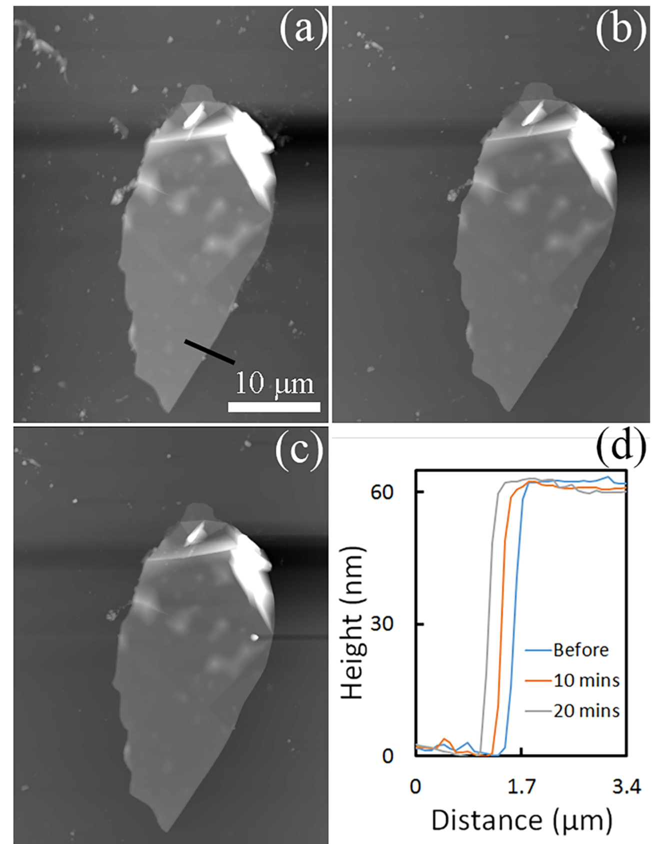

FIG. 3. AFM images of a thick graphene flake on low-resistivity Si (a) before, (b) after 10 min, and (c) after 20 min of exposure. (d) Height profiles of the flake before irradiation, after 10 min, and after 20 min of exposure along the black line drawn on (a). The scale bar in (a) is the scale for images (a)–(c).

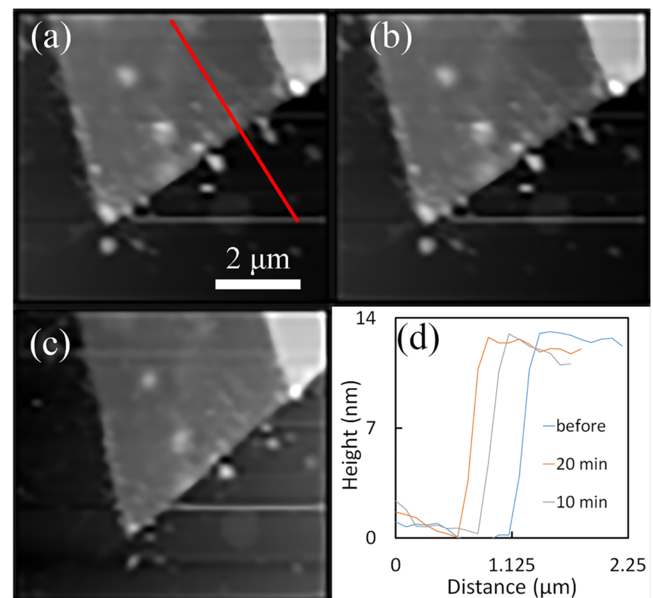

FIG. 4. AFM images of a thin graphene flake on low-resistivity Si (a) before irradiation, (b) after 10 min, and (c) after 20 min of exposure. (d) Height profiles of the flake before irradiation, after 10 min, and after 20 min of exposure along the red line drawn on (a). The scale bar on (a) is the scale for images (a)–(c).

gas to remove H_2O adsorbates or any possible contamination on the sample surfaces. In Ref. 15, we reported etching of exfoliated graphene on SiO_2 by LE electron irradiation in which the samples were preheated *in situ* at a pressure of 1×10^{-5} Torr for 1 h at a temperature of 400 °C before irradiation. As discussed in Ref. 15, it has been reported that heating multilayer graphene at 150 °C desorbs H_2O, CO_2, and N_2 and heating at 200 °C desorbs O_2. These experiments also support that oxygen does not come from preadsorbed molecules on the sample surface.

However, these results do not exclude the possibility that the conductivity of the substrate plays a role in the etching. As previously mentioned, electrically isolated graphene flakes on a dielectric material such as SiO_2, when irradiated by electrons, tend to charge negatively, which may lead to He^+ ion bombardment. It was not possible to measure the charging of the substrate. However, the charging can be inferred from the total emitted electron yield. The charging of a sample is determined by the total emitted electron yield $(\delta + \eta)$, where δ is the secondary electron yield and η is the backscattered electron yield. If $(\delta + \eta) > 1$, the sample charges positively, and if $(\delta + \eta) < 1$, the sample charges negatively. For 10 nm thick SiO_2/Si and incident electrons of about 50 eV, δ is about 1.5, and so SiO_2 would charge positively.[21] However, graphene has been measured to have an ultralow δ of around 0.10.[22] The backscattered yield, η, increases with atomic weight and for a low atomic weight atom such as C is about 0.1.[23] Thus, we propose that graphene would charge negatively with respect to the surrounding substrate if irradiated with electrons and electrically isolated on a dielectric substrate. We note that when $(\delta + \eta) < 1$ and negative charging occurs, samples can charge to as much as the primary electron beam potential.[24] The negative charge on the graphene would attract the He^+ ions, the main He ion species. As discussed previously, He^+ ion bombardment causes the greatest amount of defects and sputtering at low energies.[14] Thus, the defects that are necessary for etching to occur may be produced by the He ions instead of the incident electrons. We note that in Ref. 2, it was reported that amorphous carbon films up to 20 nm in thickness on SiO_2 also etched under LE electron irradiation at 50–200 eV. This phenomenon was not well understood since the mean free path of electrons is on the order of 0.48 nm,[19] as previously discussed. Amorphous carbon films also have a low secondary electron yield of about 0.65–0.9 for freshly made samples in this energy range.[25] We propose the He^+ ion bombardment may be responsible for the etching.

To test this hypothesis, we tested if the presence of oxygen in a conducting substrate would induce etching. On a conducting substrate, graphene would not be electrically isolated and would not build up a negative charge. For that, we irradiated graphene exfoliated on an ITO substrate. We expect oxygen to be dissociated from the ITO by the mechanism discussed previously.[13] Additionally, it has been reported that oxides with a cation and anion Pauling electronegativity difference of >1.7 are highly susceptible to O^+ dissociation and desorption due to LE electron beam irradiation.[13,26] This criterion is met by a variety of materials including SiO_2 and Al_2O_3.[13,26] ITO is a mixture of In_2O_3, which has an electronegativity difference of 1.8, and SnO_2, which has an electronegativity difference of 1.7, and thus also satisfies this criterion. Figure 5(a) is an optical image of a graphene flake on ITO before electron beam irradiation, and Fig. 5(b) is the corresponding AFM image. Figure 5(c) is an AFM image of the same flake after 10 min under irradiation at the same conditions as all the previous exposures. Finally, Fig. 5(d) shows the height profiles of both the AFM images denoted by the line in Fig. 5(b). As in the previous figures, the height profile lines are displaced horizontally for clarity. The heights before and after the irradiation are the same, which indicates that exfoliated graphene on ITO did not etch. We also collected data for a thin area of graphene on ITO, with Figs. 6(a) and 6(b) showing an optical and AFM image of a 7 nm thick flake, respectively. Figures 6(c) and 6(d) show optical and AFM images, respectively, of the flake after 10 min of irradiation. Figure 6(e) superimposes the heights of the flake taken along the line from Fig. 6(b) before and after the irradiation and is displaced horizontally for clarity. The heights for both the AFM images are the same, and so it is concluded that thin graphene also does not etch on ITO. In the ITO experiment, any excess electrons on the graphene flake are conducted through the substrate and exit to ground, failing to build a negative charge on the graphene. As a result, there would be no He^+ ion bombardment. The oxygen that we expect to be dissociated fails to react with and etch the multilayer graphene in the same

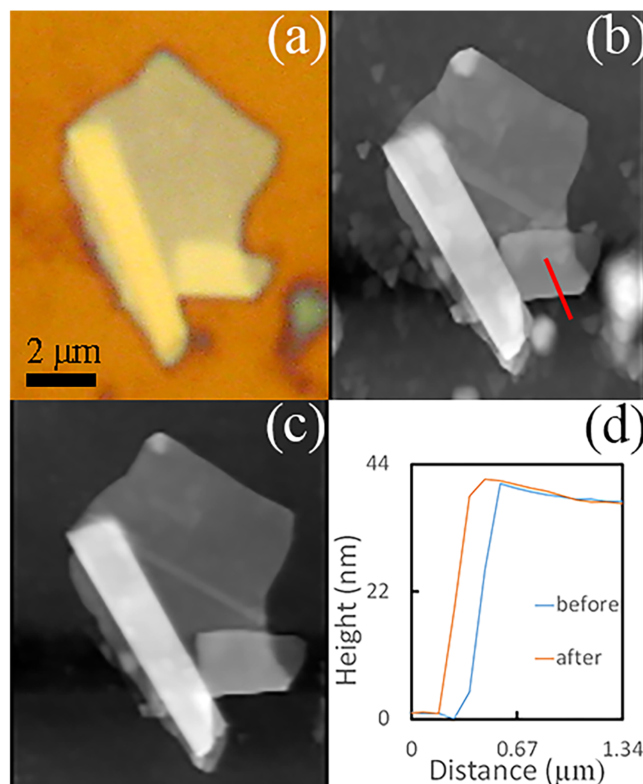

FIG. 5. (a) Optical image of a thick graphene flake on ITO. (b) and (c) AFM images of the flake before and after 10 min of irradiation, respectively. (d) Height profiles for the flake before and after irradiation along the red line drawn on (b). The scale bar on (a) is the scale for images (a)–(c).

magnitude as we see for the SiO_2 substrate. Therefore, we conclude that oxygen and defects caused by the electron irradiation may not necessarily catalyze the etching of graphene. Additionally, it seems that the conductivity of the substrate may play a role in the mechanism; specifically, conducting substrates, regardless of the availability of oxygen, do not cause etching of exfoliated graphene. We believe that this is so because graphene on conducting substrates only experiences LE electron irradiation, and any defects that LE electrons produce in the graphene are not etched by oxygen. We propose that only when He^+ ions are accelerated due to the negative charge buildup in graphene on dielectric substrates will the proper defects form that allow oxygen to etch the graphene. This proposition is consistent with our experiments as graphene on SiO_2 experiences ion bombardment and oxygen dissociates from SiO_2 and therefore etches graphene, but low-resistivity Si and ITO do not etch because there is no charge buildup in the graphene and therefore no ion bombardment.

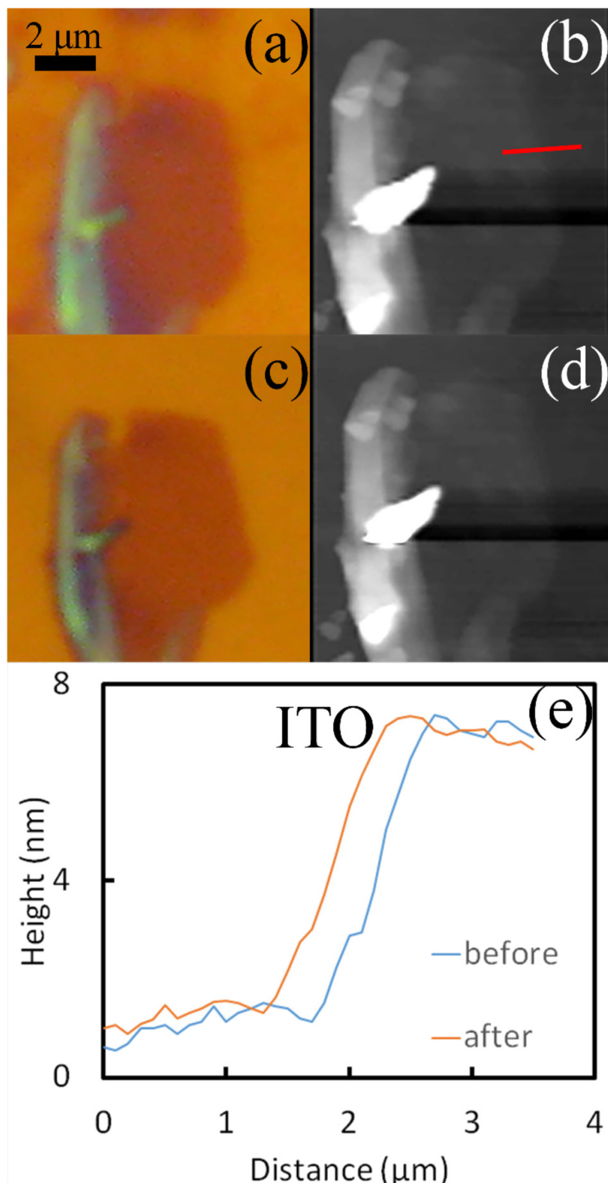

FIG. 6. (a) Optical image of a thin graphene flake on ITO and (b) the corresponding AFM image. (c) Optical image of the same flake after 10 min of irradiation and (d) the corresponding AFM image. (e) Height profiles for the flake before and after irradiation along the red line drawn on (b). The scale bar on (a) is the scale for images (a)–(d).

The final two substrates we irradiated aim to provide instances where electrically isolated graphene on a substrate without oxygen will etch. For this purpose, we used SiC, a dielectric material without any oxygen, and higher resistivity Si, which will provide insights into the effect of substrate resistivity on etching. For both the samples, only thin graphene flakes were analyzed as it is easier to see height changes. One may speculate that thin graphene flakes on any substrate would etch, but our results from the low-resistivity Si in which the thinner pieces did not etch show otherwise. Figure 7(a) is an optical image of the graphene flake on SiC before irradiation. We note that few-layered graphene flakes exfoliated on SiC are light shades of green, and thicker flakes have a darker color of green. Figure 7(b) is the AFM image corresponding to the graphene sample from Fig. 7(a). Figure 7(c) is an optical image of the same graphene flake shown in Fig. 7(a) after 10 min of electron beam irradiation under the same conditions as all the previous exposures. It is

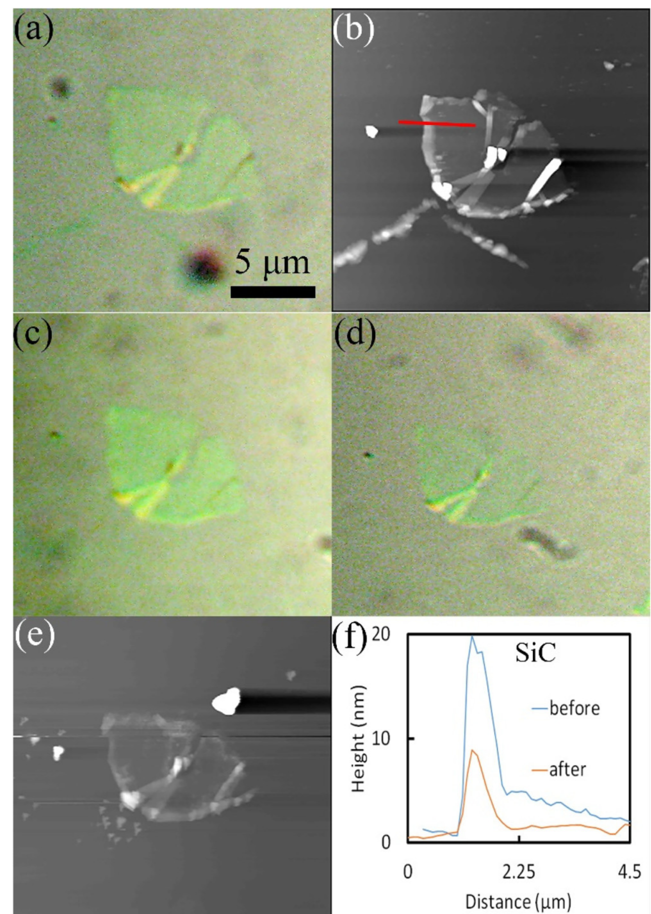

FIG. 7. (a) Optical image of a thin graphene flake exfoliated on SiC and (b) the corresponding AFM image. (c) and (d) Optical images of the same flake after 10 min irradiation and (d) 20 min irradiation. (e) AFM image corresponding to (d). (f) Height profiles for the flake before and after 20 min of irradiation along the red line drawn on (b). The scale bar on (a) is the scale for images (a)–(e).

noted that the color of the graphene flake is of a slightly lighter shade of green than that of Fig. 7(a). Figure 7(d) is another optical image of the flake after an additional 10 min of irradiation. The color of the graphene sample appears to be of an even lighter shade of green. Figure 7(e) is an AFM image of the flake after the combined 20 min of irradiation, corresponding to the graphene flake from Fig. 7(d). Figure 7(f) shows the height profiles along the line in the AFM image shown in Fig. 7(b). We believe that the ridge on the border of the graphene sample is either polymer from the tape or a wrinkle in the graphene. However, the inner region is ascribed to graphene. The height profile for the flat graphene in the inner region of the sample before irradiation is 2–4 nm higher than the height profile for the region after 20 min of irradiation, indicating that LE electron irradiation on SiC etches exfoliated graphene, albeit not nearly as much as SiO_2. Therefore, due to the fact that graphene on SiC etches despite SiC not having oxygen in the substrate, we propose that He^+ ion bombardment causes the etching by the mechanisms discussed previously of sputtering and vacancy formation.[14] Additionally, due to the fact that SiC etches much less compared to SiO_2, we propose that oxygen reacting at defects etches graphene at a much faster rate than only ion bombardment. We did not measure the density of metastable He species in the chamber. Therefore, we did not consider the effects of metastable He in our experiment.

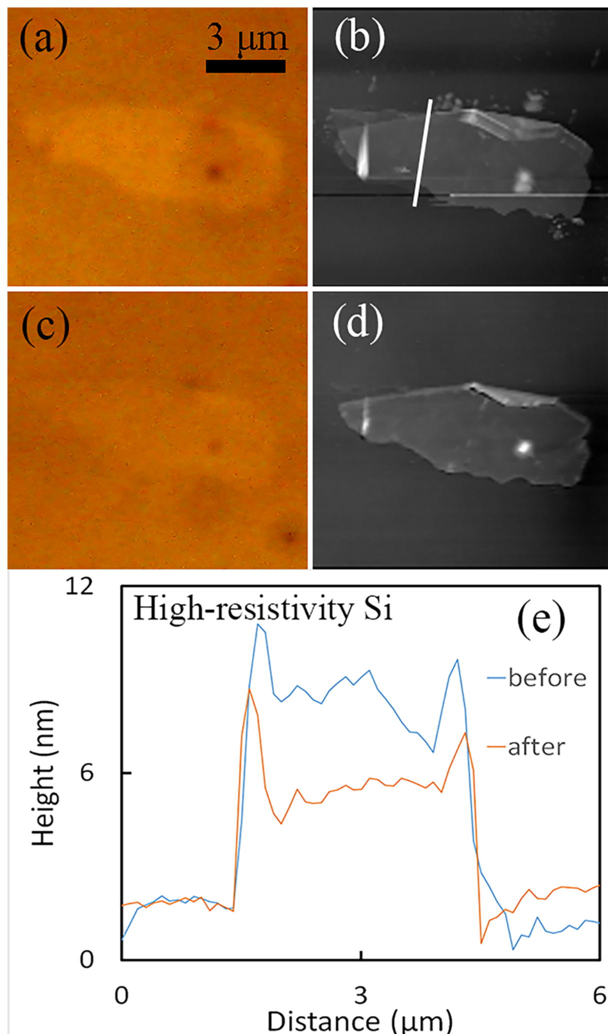

Fig. 8. (a) Optical image of a thin graphene flake exfoliated on high-resistivity Si and (b) the corresponding AFM image. (c) Optical image of the same flake after 10 min of irradiation and (d) the corresponding AFM image. (e) Height profiles for the flake before and after irradiation along the white line drawn on (b). The scale bar on (a) is the scale for images (a)–(d).

To further investigate the relationship between etching and substrate resistivity, we irradiated graphene exfoliated on the higher resistivity 10 Ω cm Si substrate. Since the resistance is higher, the incident electrons on the graphene would produce a higher negative potential than for the low-resistivity Si. Figure 8(a) is an optical image of a 10 nm thin flake, and Fig. 8(b) is the corresponding AFM image. Figure 8(c) is an optical image of the same flake after 10 min of irradiation. The flake appears fainter than the flake of Fig. 8(a), indicating that the flake has thinned. Figure 8(d) is the corresponding AFM image. Figure 8(e) shows the height profiles of the flake before and after the irradiation along the line shown in Fig. 8(b). The height has decreased about 3–5 nm after the irradiation, suggesting that the higher the resistivity of the Si, the more the exfoliated graphene on the substrate etches. The increased damage on the graphene is seen on the higher resistivity Si but not on the low-resistivity Si. This corroborates our hypothesis that the substrates with greater resistivity allow negative charge to build up on the graphene creating an electric field which attracts He^+ ions. Spinney *et al.*[27] and Sommer *et al.*[28] reported etching of carbon films and suspended graphene monolayers, respectively, using gas-assisted focused electron beam etching at beam energies of 5 and 30 keV, respectively, with water vapor as the gas. It was proposed that etching occurred due to dissociation of water adsorbed on the sample surface resulting in oxidation of carbon. We note that carbon films contain defects, and the suspended graphene layer was reported in Ref. 28 to display a Raman D peak after etching, indicating the process induced defects. Thus, these experiments do not contradict our conclusion that oxygen reacts with defects formed by He^+ ions.

IV. SUMMARY AND CONCLUSIONS

We propose that graphene exfoliated on SiO_2 experiences etching from the top of the sample rather than from the bottom. This is supported by our observation that thinner regions of graphene do not etch at a faster rate than thicker regions. We propose that oxygen is dissociated from the surrounding SiO_2 substrate and diffuses to above the graphene sample and etches it. This is in contrast to a previously proposed model[2] in which oxygen dissociates at the graphene/SiO_2 interface and etches the graphene from below. We find that exfoliated graphene does not etch on low-resistivity Si, in support of the oxygen dissociation hypothesis. We further find that etching does not occur on ITO, where etching would be expected from the previously proposed model[2] since ITO contains oxygen. However, etching occurs on higher resistivity Si and SiC, although much less than on SiO_2. We attribute this to negative charge build up on the graphene flakes that accelerates He^+ ions near the surface and causes sputtering

and defect formation. As a result of the defects formed by the He^+ ions, oxygen is able to react with and etch graphene. This is in contrast to the previous model[2] in which electrons cause the necessary defects to allow oxygen to etch graphene. We propose that graphene will etch on dielectric substrates, and if oxygen dissociates from the dielectric substrate, the etching occurs at a much higher rate. If there is no oxygen in the dielectric substrate, etching still occurs due to sputtering of the graphene by He^+ ions. We propose that conducting substrates, however, will not result in etching regardless of the dissociation of oxygen due to lack of He^+ ion bombardment.

ACKOWLEDGMENTS

The authors thank Murthada Adewole and Yuankun Lin for helpful discussions.

[1]K. S. Novoselov, A. K. Geim, S. Morozov, D. Jiang, M. Katsnelson, I. Grigorieva, S. Dubonos, and A. A. Firsov, Nature **438**, 197 (2005).
[2]C. Chen, C. Wang, and D. Diao, Appl. Phys. Lett. **109**, 053104 (2016).
[3]C. M. Seah, B. Vigolo, S. P. Chai, and A. R. Mohamed, Carbon **105**, 496 (2016).
[4]L. Xie, L. Jiao, and H. Dai, J. Am. Chem. Soc. **132**, 14751 (2010).
[5]I. Childres, L. A. Jauregui, J. Tian, and Y. P. Chen, New J. Phys. **3**, 025008 (2011).
[6]X. Yang, S. Tang, G. Ding, X. Xie, M. Jiang, and F. Huang, Nanotechnology **23**, 025704 (2011).
[7]H. Al-Mumen, F. Rao, W. Li, and L. Dong, Nanomicro Lett. **6**, 116 (2014).
[8]W. S. Lim *et al.*, Carbon **50**, 429 (2012).
[9]G. H. Han *et al.*, ACS Nano **5**, 263 (2011).
[10]M. D. Fischbein and M. Drndić, Appl. Phys. Lett. **93**, 113107 (2008).
[11]M. C. Lemme, D. C. Bell, J. R. Williams, L. A. Stern, B. W. Baugher, P. Jarillo-Herrero, and C. M. Marcus, ACS Nano **3**, 2674 (2009).
[12]F. Banhart, Rep. Prog. Phys. **62**, 1181 (1999).
[13]M. L. Knote and P. J. Feibelman, Phys. Rev. Lett. **40**, 964 (1978).
[14]O. Lehtinen, J. Kotakoski, A. V. Krasheninnikov, A. Tolvanen, K. Nordlund, and J. Keinonen, Phys. Rev. B **81**, 153401 (2010).
[15]J. D. Jones, R. K. Shah, G. F. Verbeck, and J. M. Perez, Small **8**, 1066 (2012).
[16]J. D. Jones, W. D. Hoffmann, A. V. Jesseph, C. J. Morris, G. F. Verbeck, and J. M. Perez, Appl. Phys. Lett. **97**, 233104 (2010).
[17]M. Morita, T. Ohmi, E. Hasegawa, M. Kawakami, and M. Ohwada, J. Appl. Phys. **68**, 1272 (1990).
[18]Thin Film Devices, Inc., 1180N. Tustin Ave., Anaheim, CA 92897.
[19]S. Tanuma, C. J. Powell, and D. R. Penn, Surf. Interface Anal. **37**, 1 (2005).
[20]M. Topsakal, H. Şahin, and S. Ciraci, Phys. Rev. B. **85**, 155445 (2012).
[21]J. J. Fijol, A. M. Then, G. W. Tasker, and R. J. Soave, Appl. Surf. Sci. **48–49**, 464 (1991).
[22]J. Luo, P. Tian, C. T. Pan, A. W. Robertson, J. H. Warner, E. W. Hill, and A. D. Briggs, ACS Nano **5**, 1047 (2011).
[23]L. Reimer, *Springer Series in Optical Sciences* (Springer, Berlin, 1998), Vol. 45, p. 135.
[24]M. T. Postek and A. E. Vladár, Proc. SPIE **9636**, 963605 (2015).
[25]A. Santos, N. Bundaleski, B. J. Shaw, A. G. Silva, and O. M. N. D. Teodoro, Vacuum **98**, 37 (2013).
[26]C. G. Pantano and T. E. Madey, Appl. Surf. Sci. **7**, 115 (1981).
[27]P. S. Spinney, D. G. Howitt, S. D. Collins, and R. L. Smith, Nanotechnology **20**, 465301 (2009).
[28]B. Sommer, J. Sonntag, A. Ganczarczyk, D. Braam, G. Prinz, A. Lorke, and M. Geller, Sci. Rep. **5**, 7781 (2015).